Consistency of post-Newtonian waveforms with numerical relativity

John G. Baker,[1] James R. van Meter,[1,2] Sean T. McWilliams,[3] Joan Centrella,[1] and Bernard J. Kelly[1]

[1] *Gravitational Astrophysics Laboratory, NASA Goddard Space Flight Center, 8800 Greenbelt Rd., Greenbelt, MD 20771, USA*
[2] *Center for Space Science & Technology, University of Maryland Baltimore County, Physics Department, 1000 Hilltop Circle, Baltimore, MD 21250*
[3] *University of Maryland, Department of Physics, College Park, MD 20742, USA*

(Dated: December 5, 2006)

General relativity predicts the gravitational radiation signatures of mergers of compact binaries, such as coalescing binary black hole systems. Derivations of waveform predictions for such systems are required for optimal scientific analysis of observational gravitational wave data, and have so far been achieved primarily with the aid of the post-Newtonian (PN) approximation. The quality of this treatment is unclear, however, for the important late inspiral portion. We derive late-inspiral waveforms via a complementary approach, direct numerical simulation of Einstein's equations, which has recently matured sufficiently for such applications. We compare waveform phasing from simulations covering the last ~ 14 cycles of gravitational radiation from an equal-mass binary system of nonspinning black holes with the corresponding 3PN and 3.5PN orbital phasing. We find agreement consistent with internal error estimates based on either approach at the level of one radian over ~ 10 cycles. The result suggests that PN waveforms for this system are effective roughly until the system reaches its last stable orbit just prior to the final merger.

PACS numbers: 04.25.Dm, 04.25.Nx 04.30.-w 04.30.Db, 95.30.Sf, 97.60.Lf

Compact astrophysical binaries spiral together due to the emission of gravitational radiation. Calculating the dynamics of these systems, and the corresponding gravitational waveforms, has been a central problem in general relativity for several decades. With first-generation interferometric detectors such as LIGO, VIRGO,and GEO600 now operating, and development moving forward on the space-based LISA mission, the need for accurate and reliable waveforms for gravitational wave data analysis has become urgent.

Post-Newtonian (PN) methods, based on expansions in the parameter $\epsilon \sim v/c$, have been the major analytic tool used to calculate the system dynamics and waveforms during the early part of the inspiral, when the binary components are relatively widely separated and thus have a small orbital frequency [1]. Currently, gravitational wave data analysis for binary inspiral relies on waveforms derived from PN methods [2]. The current predicted orbital phase is available up to $O(\epsilon^7)$, which is referred to as 3.5PN order. However the convergence properties of the PN sequence are not well understood, and it is not yet clear how well PN predictions work late in the inspiral when frequencies are high.

Numerical relativity, in which the full set of Einstein's equations is solved on a computer, is needed to handle the final stages of the binary evolution, when the components inspiral rapidly and merge. Recently, there has been dramatic progress in the use of numerical relativity to simulate the final inspiral and merger of black holes [3, 4, 5, 6, 7, 8, 9, 10, 11]. These breakthroughs have allowed numerical simulations with increasingly wider initial separations, producing longer wavetrains. Linking such simulations with the PN calculations and comparing their waveforms in the late inspiral regime is a pressing concern of gravitational wave data analysis.

We have carried out numerical simulations of a merging equal-mass, nonspinning black-hole binary of sufficient duration to conduct meaningful comparisons with the PN approximation. The black holes start on nearly circular orbiting trajectories $\sim 1200M$ before merger, where M refers to the mass that the system would have had when the black holes were still far apart, before radiative losses were significant. M is related to time by $M \equiv 5\times10^{-6}s(M/M_\odot)$. In this *Letter*, we quantitatively compare crucial phasing information in the our numerical simulation waveforms with phasing in PN waveforms, finding striking agreement.

The numerical simulations were performed using the moving puncture method [5, 6, 12]. We use fourth-order Runge-Kutta time integration, fourth-order accurate finite spatial differencing, and second-order-accurate initial data. Adaptive mesh refinement is used to resolve both the dynamics near the black holes and the propagation of the gravitational waves [8]. We performed physically equivalent runs at three different maximum resolutions: low ($3M/64$), medium ($3M/80$), and high ($M/32$). We find fourth-order convergence of the Hamiltonian constraint, and better than second-order convergence of the momentum constraints during the runs.

The simulations begin at an angular gravitational wave frequency $\omega \sim 0.051M^{-1}$. The frequency then sweeps upward through roughly an order of magnitude while the black holes undergo ~ 7 orbits, thus producing ~ 14 gravitational wave cycles before merger. For such long-lasting simulations, the primary consideration in providing a realistic initial data model is to set up the orbiting black holes with minimal eccentricity, as gravitating binary systems of comparable-mass objects are expected to

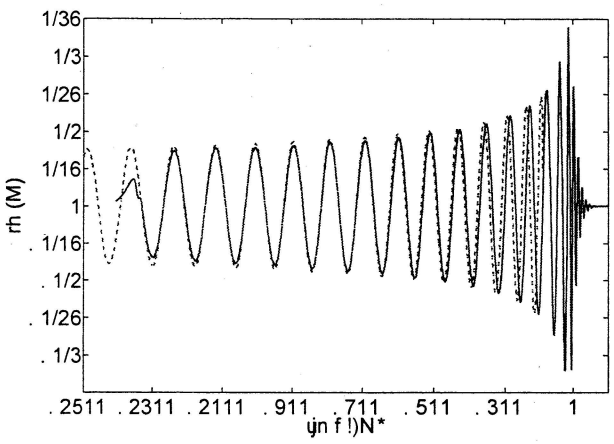

FIG. 1: Gravitational strain waveforms from the merger of equal-mass Schwarzschild black holes. The solid curve is the waveform from the high resolution numerical simulation, and the dashed curve is a PN waveform with 3.5PN order phasing and 2.5PN order amplitude accuracy. Time $t = 0$ is the moment of peak radiation amplitude in the simulation.

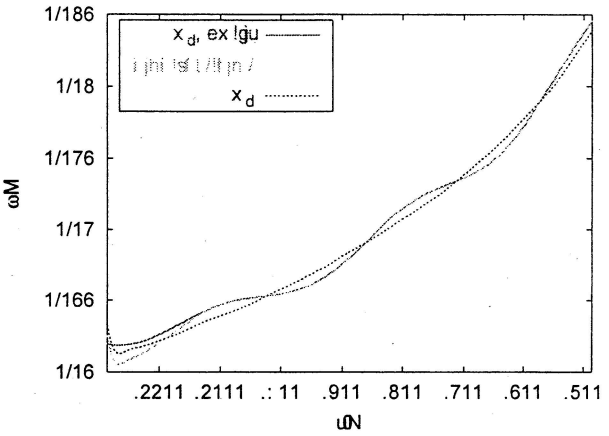

FIG. 2: Fit to estimate eccentricity in the high resolution run. The dashed (green) curve is the numerically observed frequency. The solid (red) curve is a fit to a secular increase with time with a sinusoidal perturbation caused by the eccentricity. The dotted (blue) curve is the "de-eccentrized" secular trend ω_c.

circularize rapidly through the emission of gravitational radiation. We have selected an initial black hole configuration with relatively little eccentricity of less than one percent, as measured below.

Fig. 1 shows a comparison of gravitational wave strain generated by our highest-resolution numerical run and that predicted by the PN approximation with 3.5PN phasing and 2.5PN (beyond leading order) amplitude accuracy. The waves are based on the dominant $l = 2, m = 2$ spin-weighted spherical harmonic of the radiation, and represent an observation made on the system's equatorial plane, where only one polarization component contributes to the measured strain. The initial phase and initial time of the waves have been adjusted so that the frequency and phase for each waveform agree early in the simulation, at $t = -1000M$. We will quantitatively study the evident phase agreement below.

To conduct comparisons with PN calculations, we need to extract an instantaneous gauge-invariant polarization phase ϕ and angular frequency ω from our simulations. These are derived from the first time-derivative of the gravitational wave strain, which is a robust quantity in the numerical data. This frequency corresponds to the sweep rate of the polarization angle of the circularly polarized gravitational wave that can be observed on the system's rotation axis.

We define eccentricity as deviation from an underlying smooth, secular trend. We obtain a monotonic "secular" frequency-time relation by modeling the frequency ω as a fourth-order monotonic polynomial $\omega_c(t)$, plus an eccentric modulation in the waveform angular frequency, $d\omega(t)$, of the form $d\omega(t) = \omega(t) - \omega_c(t) = A\sin(\Phi(t))$, where $\Phi(t)$ is a quadratic function of time. The fitting procedure is illustrated in Fig. 2, which shows the original numerical frequency $\omega(t)$, the fit, and $\omega_c(t)$. Fitting this data yields $A = 8(\pm 1) \times 10^{-4}$. For Keplerian systems, conserved angular momentum is proportional to $r^2\omega$ so the (radial) eccentricity corresponds to half the fractional amplitude of frequency modulations: $e = A/(2\omega)$. In our case the eccentricity starts near 0.008, decreasing by a factor of three by the time $\omega_c M \sim 0.15$. We will compare our simulation with non-eccentric PN calculations, with the expectation that small eccentricities have minimal effect on the important underlying secular trend in the rate at which frequency sweeps up approaching merger.

The phasing of the waveform is critical for gravitational wave observation. For data analysis, the optimal methods for both detection and parameter estimation rely on matched filtering, which employs a weighted inner product that can be expressed in Fourier space as $< h, s >= \int (\tilde{h}^*(f)\tilde{s}(f) + \tilde{h}(f)\tilde{s}^*(f))/S_n(f)df$, where h is the template being used, s is the signal being analyzed, and S_n is the one-sided power spectral density of the detector's noise [13]. A template that maximizes $< h, s >$ will provide an optimal filter. While a template with time-varying amplitude can emphasize some portions of a signal and not others, the crucial factor is the relative phasing of the template and signal. The inner product will cease to accumulate in sweeping through frequency if the template and the signal evolve to be out of phase with each other by more than a half-cycle, decreasing the effectiveness of the procedure.

Our key objective is to compare phasing between nu-

merical and PN waveforms. To avoid issues with timing alignment, we will compare phases as a function of polarization frequency, which corresponds to twice the orbital frequency in the PN case. For circular inspiral this frequency should grow monotonically in time, with the frequency ω_c providing a physical reference of the "hardness" of the tightening binary.

Circular inspiral phasing information is typically derived in PN theory by imposing an energy balance relation to deduce the rate at which ω_c evolves from the radiation rate at a specified value of ω_c [1]. Though not strictly derived in the PN context, this physically sensible condition currently allows the determination of the chirp rate $\dot{\omega}_c(\omega_c)$ (or something equivalent) up to 3.5PN order [14]. From such a relation information about phase and time are determined by integrating $d\phi/d\omega_c = \omega_c/\dot{\omega}_c$ and $dt/d\omega_c = 1/\dot{\omega}_c$. The phasing information can be represented by any one of several relations between phase, frequency and time. Various approaches take the PN-expanded representation of one of these relations as the PN "result" for waveform phasing [1, 3, 14]. We consider both the PN expansion of the chirp rate, numerically integrated as needed, as well as the PN expansion of the phase.

For the purpose of comparison with our numerical simulations, we invert the monotonic function $\omega_c(t)$ to obtain the phase as a function of frequency: $\phi(\omega_c) = \phi(t(\omega_c))$. Note that the effect of eccentricity is not removed from ϕ, though the "circularized" frequency ω_c does provide the abscissa according to which phases are compared in the different treatments.

Fig. 3 shows the wave phases; here the phases are adjusted by addition of a constant so that each phase vanishes at $\omega_c M = 0.054$, corresponding to the time $1000M$ before the radiation merger peak in the high resolution numerical simulation. The sequence of numerical results converges at fourth-order (verified in Fig. 4), allowing us to project by Richardson extrapolation to a fifth-order accurate result (thick solid line in Fig.3).

In Fig. 3 we compare the numerical simulation results with two versions of PN-phasing, based on either the PN expansion of the phase or on the numerically integrated PN expansion of the chirp rate. We show each of these at 3PN and 3.5PN order. While the 3PN phase seems to agree closely with the extrapolated numerical phase, the 3.5PN phase moves away, and develops an unphysical negative slope after $\omega_c M \sim 0.15$. The agreement of the extrapolated numerical result with the integrated PN chirp rate improves from 3PN to 3.5PN, with the 3.5PN result showing striking agreement up to about $\omega_c M \sim 0.15$.

We look more quantitatively at the differences among the phases in Fig. 4. The solid curve shows the difference between our medium and high resolution results, while the dotted curve shows the difference between our low and medium resolution results, scaled such that for

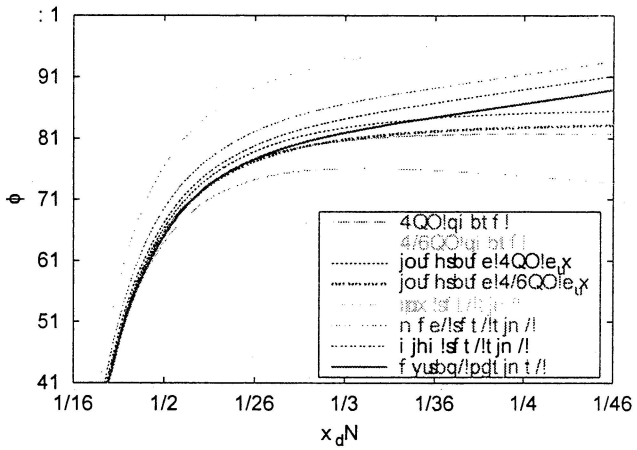

FIG. 3: Gravitational wave phase, in radians, for numerical and two versions of PN waveforms. The sequence of numerical simulation results approaches the solid curve, which agrees well with the phase obtained by numerically integrating the 3.5PN expansion of the chirp rate $\dot{\omega}_c(\omega_c)$. It also agrees with the PN expansion of $\phi(\omega_c)$ at 3PN order though the 3.5PN order curve reaches an unphysical maximum value near $\omega_c M \sim 0.2$.

fourth-order convergence the curves should superpose. This is indeed demonstrated to good approximation. A good estimate for the error of the phase in the high resolution run is given by its difference from the phase obtained by Richardson extrapolation; this comes out to $\sim 93\%$ of the med-high (solid) curve shown in the figure. Note that the cumulative errors in the numerically-generated waveforms accrue primarily before the orbital frequency $\omega_c M = 0.1$. (This makes sense generally since the simulations spend much more time at lower frequencies.)

Without monotonic convergence between the 2PN, 2.5PN and 3PN at the frequencies considered here, it is difficult to estimate errors in the PN phase. Nonetheless we tentatively take the difference between the integrated 3PN and 3.5PN chirp rates, shown by the dashed line in Fig. 4, as a measure of PN errors.

The trend in the slope of these error curves indicates the rate at which phase error accumulates, as independently estimated within each approach. Fig. 4 suggests that phasing errors for our high resolution simulation accumulate more quickly than PN phasing errors for $\omega_c M \lesssim 0.08$ ($t \lesssim -300M$), with the numerical simulation phasing being more accurate than PN at higher frequencies. In both cases, the phase error accumulates to roughly two radians by $\omega_c M \sim 0.2$ as the black holes begin to plunge together.

We now address the central objective of this letter, a quantitative comparison of numerical and PN phasing results. We compare the Richardson-extrapolated phase, our best simulation estimate, with the integrated 3.5PN chirp rate result. The difference is shown in the solid

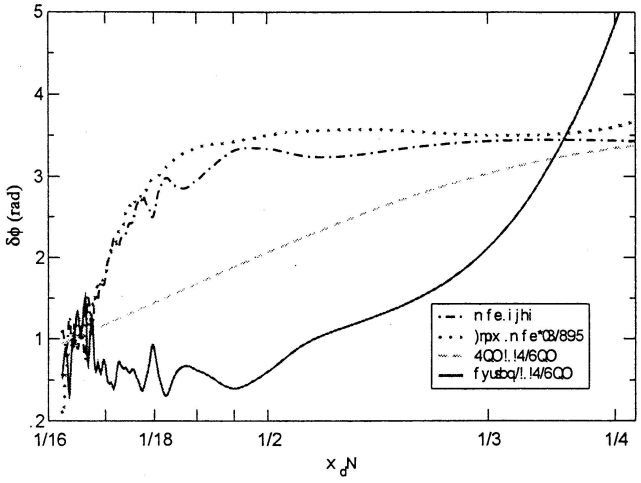

FIG. 4: Gravitational wave phase error estimates. Differences between phasing from the integrated 3.5PN chirp rate and Richardson extrapolation from the numerical simulations (solid curve) are small, and are consistent with internal error estimates for the numerical simulation results and the PN sequence.

curve of Fig. 4. Note that the phase differences between the PN and numerical results (solid curve) accumulate less rapidly than the estimated errors in either the high resolution simulation or the 3.5PN results over much of the frequency range shown. This indicates that the numerical and post-Newtonian predictions appear to be converging to a common answer for waveform phase, in a frequency regime where the validity of the PN predictions could not previously be assessed. The phase difference among the best estimates of the numerical and PN approaches begins to grow more significantly after about $\omega_c M \sim 0.15$ ($t \sim -70M$) occurring about a cycle before the estimated end of the binary's last stable orbit.

Through the frequency range $0.054 \lesssim \omega_c M \lesssim 0.15$ the net phase difference, measured against frequency, amounts to less than one radian, a level of error which would be tolerable in many gravitational wave data analysis applications. For most of the range studied here, the frequency-based phase differences between our high resolution simulation and the integrated 3.5PN chirp rate result seem larger than the time-based phase differences, which are evident in Fig. 1. This is because the sweep rate differences have not yet grown to a significant phase difference; the difference would become evident if the waveform was continued farther. At the higher frequency end of the waveform, the time-based differences would appear larger, unless the waveform was aligned to agree at the end of the waveform. This sensitivity to time-alignment makes frequency-based phase comparisons a more reliable indicator of phasing differences.

Our results provide a crucial cross-validation of PN waveforms from the late inspiral of binary merger, with results of new long-lasting numerical simulations. These simulations have sufficient accuracy to provide a meaningful comparison with PN waveforms over the last $t \sim 1000M$ of the coalescence, specifically addressing a binary system of equal-mass non-spinning black holes. We find phase agreement consistent with internal phase-error estimates conducted in each approach, indicating that phase accuracies within a few radians are now achievable for this part of the coalescence waveform.

We emphasize, however, that there is still much important work to be done in improving and further assessing PN and numerical simulation waveforms. Certainly we have only addressed one case in a large parameter space of potential binaries, which will inevitably include systems, such as rapidly precessing unequal-mass spinning binaries, which are harder to treat with present PN and numerical techniques. With either approach, even for our simple case, a non-negligible amount of phasing error accumulates over the range studied, and more will have accumulated at lower-frequencies addressable through the PN approximation. We expect continuing developments in numerical simulations and the pursuit of higher-order PN treatments to be crucial for developing a refined understanding of coalescence waveforms, which will be crucial in some data analysis applications for gravitational wave observations.

This work was supported in part by NASA grant O5-BEFS-05-0044. The simulations were carried out using Project Columbia at NASA Ames Research Center. J.v.M. and B. K. were supported by the NASA Postdoctoral Program at the Oak Ridge Associated Universities.

[1] L. Blanchet, Living Rev. Rel. **9** (2006), gr-qc/0202016.
[2] A. Buonanno, Y. B. Chen, and M. Vallisneri, Phys. Rev. D **67**, 024016 (2003), gr-qc/0205122v1.
[3] A. Buonanno, G. B. Cook, and F. Pretorius, unpublished (2006), gr-qc/0610122.
[4] F. Pretorius, Phys. Rev. Lett. **95**, 121101 (2005), gr-qc/0507014.
[5] M. Campanelli, C. O. Lousto, P. Marronetti, and Y. Zlochower, Phys. Rev. Lett. **96**, 111101 (2006), gr-qc/0511048.
[6] J. G. Baker, J. Centrella, D.-I. Choi, M. Koppitz, and J. van Meter, Phys. Rev. Lett. **96**, 111102 (2006), gr-qc/0511103.
[7] M. Campanelli, C. O. Lousto, and Y. Zlochower, Phys. Rev. D **73**, 061501 (2006), gr-qc/0601091.
[8] J. G. Baker, J. Centrella, D.-I. Choi, M. Koppitz, and J. van Meter, Phys. Rev. D **73**, 104002 (2006), gr-qc/0602026.
[9] M. Campanelli, C. O. Lousto, and Y. Zlochower, Phys. Rev. D **74**, 041501 (2006), gr-qc/0604012.
[10] M. Campanelli, C. O. Lousto, and Y. Zlochower, Phys. Rev. **D74**, 084023 (2006), astro-ph/0608275.
[11] J. A. Gonzalez, U. Sperhake, B. Bruegmann, M. Hannam, and S. Husa, unpublished (2006), gr-qc/0610154.

[12] J. R. van Meter, J. G. Baker, M. Koppitz, and D.-I. Choi, Phys. Rev. D **73**, 124011 (2006), gr-qc/0605030.
[13] C. Cutler, T. A. Apostolatos, L. Bildsten, L. S. Finn, E. E. Flanagan, D. Kennefick, D. M. Markovic, A. Ori, E. Poisson, G. J. Sussman, et al., Phys. Rev. Lett. **70**, 2984 (1993).
[14] L. Blanchet, A. Buonanno, and G. Faye (2006), accepted for publication in Phys. Rev. D, gr-qc/0605140.